ACS APPLIED MATERIALS & INTERFACES

Research Article

www.acsami.org

Efficient and Selective Removal of Dyes Using Imidazolium-Based Supramolecular Gels

Ni Cheng,[†] Qiongzheng Hu,[‡] Yongxian Guo,[†] Yong Wang,[§] and Li Yu*[,†]

[†]Key Laboratory of Colloid and Interface Chemistry, Shandong University, Ministry of Education, Jinan 250100, People's Republic of China

[‡]Department of Chemistry, University of Houston, Houston, Texas 77204, United States

[§]China Research Institute of Daily Chemical Industry, Taiyuan, 030001, People's Republic of China

Supporting Information

ABSTRACT: A supramolecular gel was constructed by using an imidazolium-based surfactant, *N*-cetyl-*N*′-carboxymethyl imidazolium bromide ([*N*-C_{16}, *N*′-CO_2H-Im]Br), in the DMSO/H_2O binary solvent mixtures and investigated as an adsorbent for removing dyes from aqueous solution. The self-assembled gel displays a morphology of microplatelets stacked in bilayer units with interdigitated hydrocarbon tails, and the structure remains unchanged below the sol−gel transition temperature. The gel also exhibits a strong birefringence property and excellent mechanical strength. In particular, the gels show superior performance in removal of anionic dye molecules, for example, removing 80% of eosin Y within 10 min, The constructed gels also present excellent salinity tolerance, even when the concentration of NaCl is 1000 times higher than that of the dye, and can maintain their high efficiency after 25 cycles, indicative of their promise in water treatment.

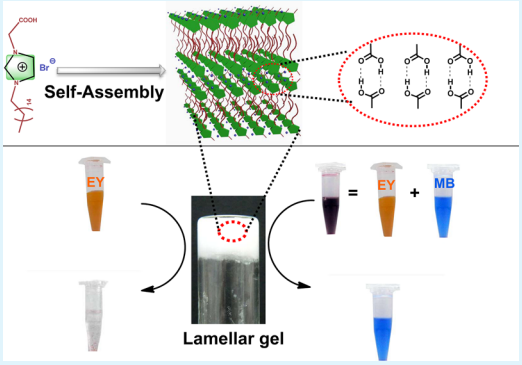

KEYWORDS: *selective removal, anionic dye, supramolecular gel, high mechanical strength*

INTRODUCTION

Highly toxic dyes will dramatically threaten environment and human health when they are directly discharged into the aqueous environment. To protect the water quality, effective removal of dyes from contaminated water is crucial. The removal methods generally include physical, chemical, and biological methods, among which the adsorption approach is widely used because of its low cost and simplicity of operation.[1,2] Various highly efficient adsorbents, such as metal−organic frameworks,[3] natural fibers,[4] and polymers[5] have been extensively applied in dye adsorption. Because the total removal of the compounds is not always required and some valuable chemicals need to be recycled in industrial waste streams,[6] advanced adsorbents offering the possibility of selective adsorption and separation of the target compounds have promising applications. For example, Jiang et al. demonstrated that hyper-branched poly(ether amine) gels could adsorb dyes selectively and dynamically separate a mixture of dyes.[7] They also reported selective adsorption and separation behavior of multiresponsive microgel to fluorescein dyes as a result of hydrophobic interactions.[8]

Compared with conventional polymeric gels formed by cross-linked covalent polymers, supramolecular gels are constructed by self-assembly of low-molecular-weight gelators (LMWGs) through noncovalent interactions.[9,10] The noncovalent interactions and designable functional groups with specific properties result in its intrinsic property's being sensitive to external stimuli, for example, temperature, mechanical stress, magnetic and electric fields, light, pH, etc.[11] Recently, supramolecular gels have been paid special attention as efficient and economic adsorbents of water-soluble dyes. The internal highly porous 3D networks provide high surface area and numerous adsorption sites, which enable easy, fast, and effective adsorption of dyes.[12] Nandi developed a Ag(I)−melamine coordination supramolecular gel that possesses the ability of selective anion dye scavenging.[13] Smith explored a hydrazide-functionalized gelator that exhibited pH-controlling dye adsorption−desorption behavior based on the interactions between host and guest molecules.[12] In general, most of the previously reported dye removal materials have displayed disadvantages, such as complex preparation, slow removal process, poor mechanical stability, and lack of regeneration. Therefore, the fabrication of adsorbents capable of selective removal and rapid separation of dyes in combination with high mechanical stability and regenerability, which are highly required for practical applications, is still challenging,.

Received: January 27, 2015
Accepted: May 1, 2015
Published: May 4, 2015

DOI: 10.1021/acsami.5b00814
ACS Appl. Mater. Interfaces 2015, 7, 10258−10265

Herein, we constructed a supramolecular gel by applying a simple heat−cool gelation process with a COOH-functionalized imidazolium-based surfactant, *N*-cetyl-*N*′-carboxymethyl imidazolium bromide ([*N*-C_{16}, *N*′-CO_2H-Im]Br), in a binary solvent mixture of DMSO/H_2O. The surfactant acts as an excellent gelator to fabricate supramolecular gels because its functional moieties, namely, imidazolium ring, alkyl chain, and COOH group, could provide rich molecular interactions, that is, $\pi-\pi$ interactions, hydrophobic interactions, and H-bonding. The constructed gels demonstrate a remarkable ability to remove dye molecules rapidly and efficiently as well as to tolerate salinity. The gels retain their excellent performance even after they are recycled 25 times and keep their original shape because of their high mechanical strength. This work shows promise of the supramolecular gels that are fabricated by the imidazolium-based surfactant for the removal of toxic dyes in contaminated water.

EXPERIMENTAL SECTION

Materials and Characterizations. The raw materials, 1-bromohexadecane (98%), imidazole (99%), and bromoacetic acid (99%), were bought from Aladdin Chemistry Co., Ltd. of China and used as received. Dyes (p.a. quality) were purchased from Sinopharm Chemical Reagent Co., Ltd. (Shanghai, China). [*N*-C_{16}, *N*′-CO_2H-Im]Br was synthesized according to the procedures described in our previous work; the synthetic approaches are indicated in Scheme 1.[14]

Scheme 1. Synthetic Procedures of [*N*-C_{16}, *N*′-CO_2H-Im]Br

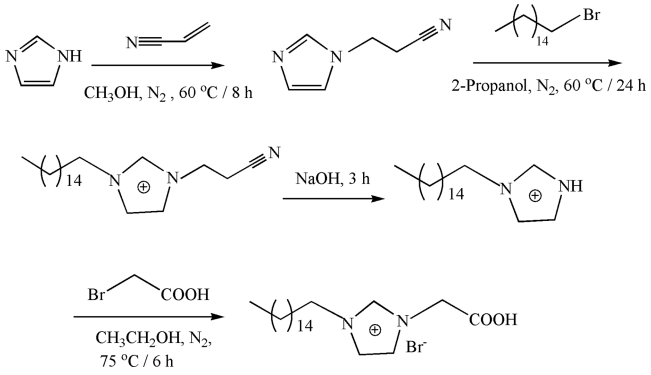

In brief, *N*-cetylimidazole was first obtained. Then bromoacetic acid was added to an ethanol solution of *N*-cetylimidazole with continuous stirring. The mixture was refluxed at 75 °C for 6 h under the protection of nitrogen. After the ethanol was removed, the residue was recrystallized five times from a methanol/ether mixture to obtain [*N*-C_{16}, *N*′-CO_2H-Im]Br. The structure was ascertained by ^{1}H NMR spectroscopy with a Bruker Avance 300 spectrometer: ^{1}HNMR (CD_3COCD_3, ppm) δ = 9.15 (s, 1 H, CH), 7.78, 7.73 (ss, 2H, CH), 5.12 (s, 2 H, CH_2), 4.20 (t, 2 H, CH_2), 1.78 (m, 2 H, CH_2), 1.23 (m, 26 H, CH_2), 0.85 (t, 3 H, CH_3).

Photographs of sample birefringence were taken by a Motic B2 polarizing optical microscope (POM) with a CCD camera (Panasonic Super Dynamic II WV-CP460). Small-angle X-ray scattering (SAXS) measurements were performed using an Anton-paar SAX Sess mc^2 system with Ni-filtered Cu Kα radiation (1.54 Å) operating at 50 kV and 40 mA. Density functional theory (DFT) calculations were carried out using the Gaussian 09 package[15] at the M06-2*X*/6-31G(d,p) level.[16,17] To consider the effects of the solvent, polarizable-continuum model (PCM)[18] was used. Frequency calculations were performed to verify that all of the optimized geometries correspond to a local minimum that has no imaginary frequency. The gel structures were characterized by scanning electron microscopy (SEM) (JMS-6700 (JEOL)). Gels were cast onto a silicon wafer and freeze-dried in a vacuum extractor at −55 °C before observation. The rheology measurements were carried out on a Haake RS75 rheometer equipped with a cone−plate sensor (Ti; diameter, 35 mm; cone angle 1°; distance 52 μm). A strain sweep experiment was carried out at deformation frequency ν = 1 Hz to determine the linear viscoelastic region. A frequency sweep was performed at a constant stress determined from the strain sweep measurements. UV−vis absorption spectra measurements were performed using a Hitachi U-4100 spectrophotometer with 2 mm path length quartz cell. The scan rate for each measurement was 300 nm·min^{-1}. Differential scanning calorimetry (DSC) measurements were performed using a Mettler Toledo DSC822^e thermal analyzer. The gel samples were conducted from −30 to 80 °C with a heating−cooling−heating cycle at a heating rate of 5 °C/min. The gel−sol phase transition temperature (T_{gel}) was identified from the maxima of the DSC melting peak.

Preparation of Gels. [*N*-C_{16}, *N*′-CO_2H-Im]Br was weighed and transferred into test tubes with a screw cap, then corresponding mixed solvents (DMSO/H_2O, wt/wt) were added to obtain the prescribed compositions (in weight percent, wt %). Subsequently, the sample was heated at 60 °C until a transparent solution was obtained and then cooled to room temperature. Upon inversion of the vial, the absence of gravitational flow was judged to be successful gelation. The lowest gelator concentration for the gel formation was assigned as the critical gelation concentration (CGC). The obtained gels can remain stable at room temperature for several months.

Dye Removal Experiments. For the typical time-dependent dye removal measurement, 1 g gels (20 wt % [*N*-C_{16}, *N*′-CO_2H-Im]Br in 40/60 (wt/wt) DMSO/H_2O binary solvent) were first prepared and then kept in contact with the aqueous dye solution (1 mL, 0.25 mM)

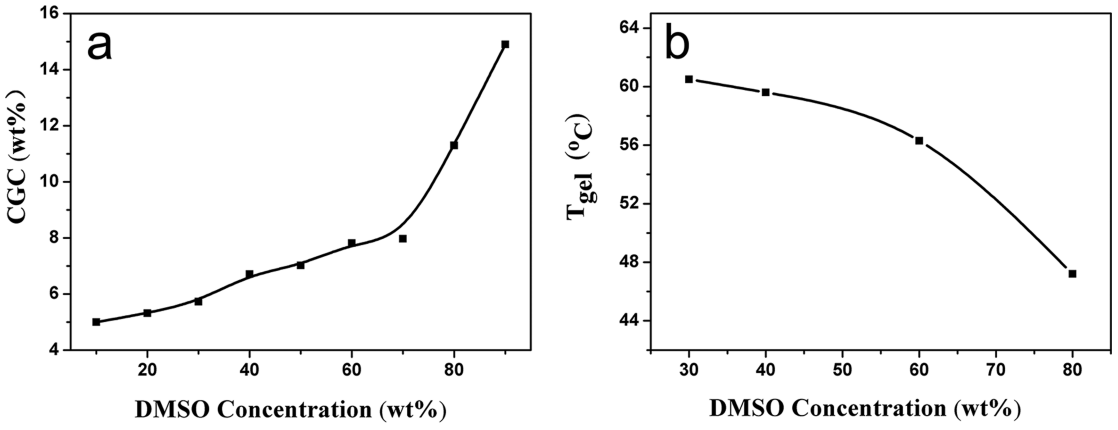

Figure 1. (a) Critical gelation concentration (CGC) at 25 °C and (b) gel melting temperature (T_{gel}) of [*N*-C_{16}, *N*′-CO_2H-Im]Br in the DMSO/H_2O mixed solvents with different DMSO concentrations.

DOI: 10.1021/acsami.5b00814
ACS Appl. Mater. Interfaces 2015, 7, 10258−10265

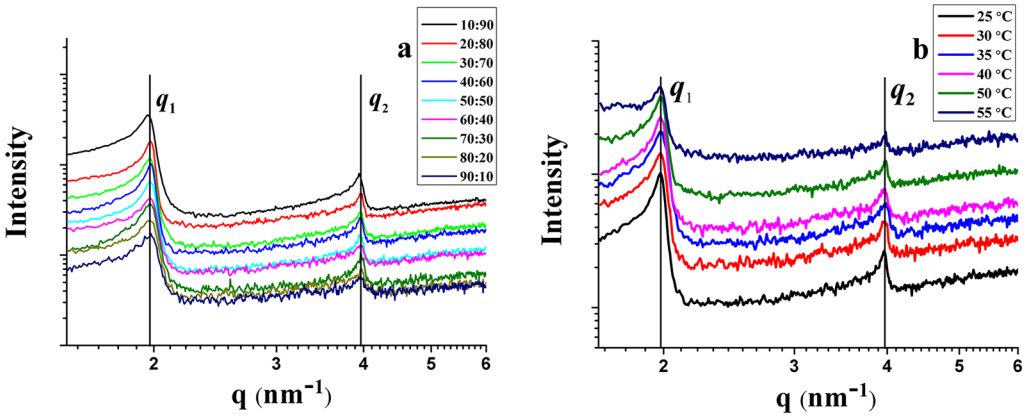

Figure 2. SAXS curves for the gels constructed by 20 wt % [*N*-C_{16}, *N*′-CO_2H-Im]Br in the DMSO/H_2O mixed solvents (wt/wt): (a) with different weight ratios at 25 °C; (b) with a ratio of 40/60 at various temperatures.

undisturbedly. For the separation of the dye mixture, 1 mL of mixed aqueous solution with a concentration of 0.25 mM for each dye was added into a 0.5 g gel sample. The residual dye concentration after removal was analyzed by UV−vis absorption spectroscopy.

RESULTS AND DISCUSSION

Gelator Efficiency and Gels Stability. Solvent selectivity can strongly affect self-assembly kinetics as well as nanostructures.[19] Through the utilization of a mixed solvent system consisting of a good solvent (DMSO) with a poor solvent (H_2O), gels can be obtained as a consequence of the delicate balance between crystallization and dissolution of the gelator.[20] As plotted in Figure 1, with increasing DMSO contents in the mixed solvents, critical gelation concentration (CGC) values show a trend of increase, and the T_{gel} decreases. This can be attributed to the increased solubility and reduced crystalline order of the gelator upon further addition of DMSO.[21]

SAXS Patterns. To investigate the detailed spatial information on the gels, small-angle X-ray scattering (SAXS) measurements were performed (Figure 2a). The SAXS patterns of the gels in binary solvent mixtures of DMSO/H_2O with different weight ratios are similar. The relative peak position q_1:q_2 is 1:2, indicative of a lamellar assembly. Average lattice spacing (d) between two lamellar structures was estimated using the Bragg's Law, $d = 2\pi/q_1$. Interestingly, d-spacing was independent of the mixed solvents (all around 31.70 Å), signifying a basic packing unit existence for the assembled gels. The d value (31.70 Å) is smaller than twice the extended alkyl chain length of [*N*-C_{16}, *N*′-CO_2H-Im]Br, but larger than the length of a single molecule (19.17 Å, from the optimized structure in Supporting Information (SI) Figure S1). Hence, the lamellar gel phase presents bilayer structures with interdigitated hydrocarbon tails.[22] To investigate the thermostability of gels, 20 wt % of [*N*-C_{16}, *N*′-CO_2H-Im]Br in DMSO/H_2O mixed solvents (40/60, wt/wt) was studied, and its SAXS plots were measured at different temperatures. As depicted in Figure 2b, in the investigated temperature range of 25−55 °C, both the two Bragg peaks and their corresponding positions (with the relative positions ratio of 1:2) remain unaltered with the elevated temperature, which suggests the gel structure remains unchanged below the sol−gel transition temperature.

Morphologies. To get visual insight into the microscopic morphology of the gels fabricated by [*N*-C_{16}, *N*′-CO_2H-Im]Br in DMSO/H_2O mixed solvents, POM and SEM measurements were performed. As shown in Figure 3a, a strong birefringence property was observed through the POM observation.

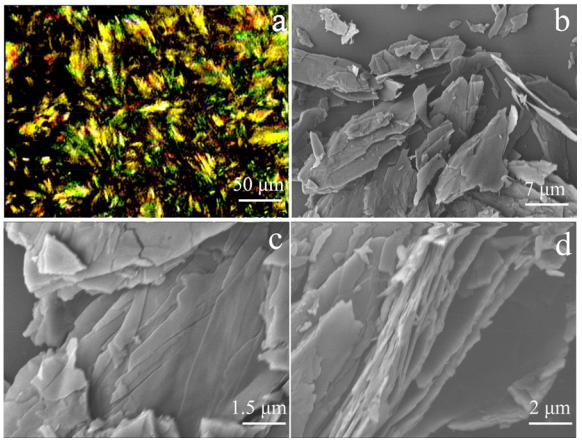

Figure 3. POM image (a) of the gels and SEM images (b−d) of the xerogels formed by 20 wt % [*N*-C_{16}, *N*′-CO_2H-Im]Br in DMSO/H_2O (40/60, wt/wt) binary solvents.

Interestingly, SEM images of the xerogel display the microplatelet-like morphology (Figure 3b). The enlarged microstructures reveal that the plates are constructed by stacked nanothin layers (Figure 3c,d). Of particular interest is that few LMWGs present such a type of self-assembly process: 0D (gelator) → 2D (nanothin layer) → 3D (platelets). In contrast, primary units of most reported molecular gels are composed of 0D → 1D (e.g., fibers, strands, tapes) → 3D (networks).[23,24] The plates with a length of several micrometers demonstrate a certain long-range order. The structural anisotropies cause the birefringence property of the gels.[25]

Rheology Properties. Figure 4a shows that both storage modulus (G') and loss modulus (G'') are initially independent of the stress, which indicates no microstructure deformation of the gels. A critical yield stress (~300 Pa), beyond which G' and G'' decrease dramatically, demonstrates the significantly high mechanical strength of the gels formed by the 20 wt % [*N*-C_{16}, *N*′-CO_2H-Im]Br in DMSO/H_2O mixture (wt/wt = 40/60). The results of frequency-dependent dynamic storage and loss moduli are presented in Figure 4b. The system shows a "solid-like" rheological behavior that meets the rheological criterion for gels.[10] G' remains larger than G'' ~1 order of magnitude and nearly frequency-independent over the entire frequency

DOI: 10.1021/acsami.5b00814
ACS Appl. Mater. Interfaces 2015, 7, 10258−10265

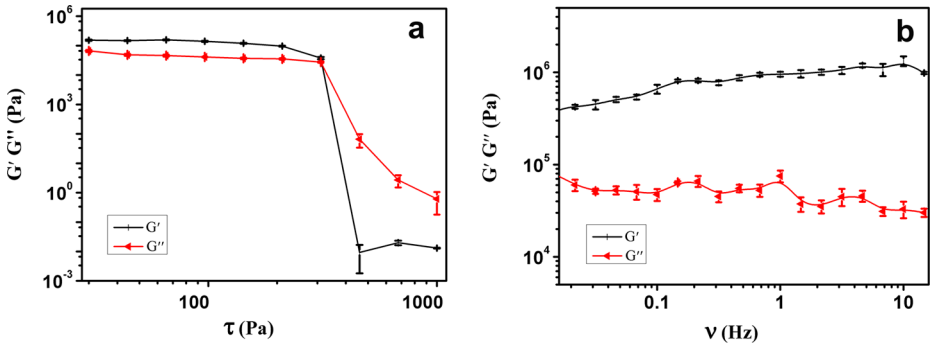

Figure 4. (a) Strain sweep lines and (b) frequency sweep lines for the gels formed by 20 wt % [*N*-C_{16}, *N*′-CO_2H-Im]Br in DMSO/H_2O (40/60, wt/wt) binary solvents.

range, displaying an elastic property. It is noteworthy that the large *G*′ value (nearly 1000 kPa) demonstrates the ordered-layer packing possesses significant stiffness to resist deformation. The *G*′ value of the gels obtained herein is much higher than that of other supramolecular gels formed by carboxylic acid LMWGs, such as enantiopure 1,2-hydroxystearic acid,[26] isomers of ketooctadecanoic acid,[19] and polymer gels (e.g., polymer cellulose acetate/*N*,*N*-dimethylacetamide/water[27] and biopolymer agarose/ionic liquids systems[28]). This exceptional rigidity property is very important for utilizing supramolecular (noncovalent) gels in various applications, such as molecular adsorption and catalysis, which require regeneration of the surface.

Gelation Mechanism. To understand the gelation mechanism, we used three analogous surfactants in an attempt to fabricate gels under the same experimental conditions (20 wt % of surfactant in DMSO/H_2O = 40/60 mixed solvents). Palmitic acid (without an imidazolium ring), [*N*-C_{10}, *N*′-CO_2H-Im]Br (possessing a shorter alkyl chain), and 1-hexadecyl-3-methylimidazolium bromide (C_{16}mimBr; lack of the COOH group) were chosen to conduct control experiments, but no gelation occurred. Therefore, $\pi-\pi$ interaction, hydrophobicity, and H-bonding provided by the imidazolium ring, alkyl chain, and COOH group are probably the driving forces for the gelation. To further understand the intermolecular H-bonding interactions between COOH groups in [*N*-C_{16}, *N*′-CO_2H-Im]Br at the molecular level, we conducted density functional theory (DFT) calculations with the cetyl chain of [*N*-C_{16}, *N*′-CO_2H-Im]Br replaced by a methyl group for computational convenience. As shown by the dashed line in SI Figure S1, there are very strong H-bonding interactions between the two carboxylic acid groups of [*N*-C_{16}, *N*′-CO_2H-Im]Br with a shortest distance of 1.65 Å. Therefore, intermolecular H-bondings between the COOH residues of the adjacent two [*N*-C_{16}, *N*′-CO_2H-Im]Br molecules can facilitate the gelation. On the basis of the lamellar packing arrangement and the driving force for the gelation, a possible gelation mechanism was proposed and is illustrated in Scheme 2. At the beginning, [*N*-C_{16}, *N*′-CO_2H-Im]Br molecules were stacked into two-dimensional bilayer units (*d* = 31.70 Å) via $\pi-\pi$ interactions between the imidazolium rings and hydrophobic interactions between the alkyl chains. Then intermolecular H-bondings between carboxylic acid groups connected these units to form three-dimensional laminar microplatelet assemblies with one layer stacking above the other. During this process, the solvent molecules were confined, and gelation was achieved.

Selective Removal of Dyes in Aqueous Solution. Toxic dye-based industrial effluents are hazardous to the ecological

Scheme 2. Proposed Aggregation Model for Gelation of [*N*-C_{16}, *N*′-CO_2H-Im]Br in Mixed DMSO/H_2O Solvents

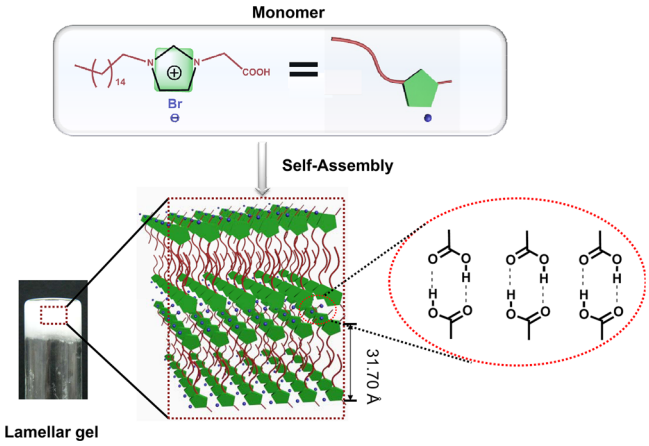

balance and environment. Therefore, seeking convenient and efficient adsorbents for decontamination of waste waters is very attractive. The dye removal behavior of the fabricated molecular gels in this work was evaluated by using different types of toxic dyes (the chemical structures are shown in Figure 5), including anionic dyes eosin Y (EY) and methyl orange (MO) and cationic dyes rhodamine 6G (R6G) and methylene blue (MB). The initial concentration of dyes was fixed at 0.25 mM, and the

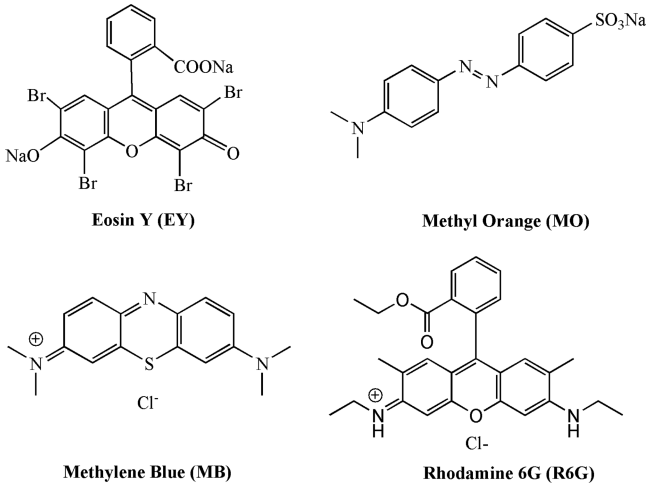

Figure 5. Molecular structures of the studied dyes.

DOI: 10.1021/acsami.5b00814
ACS Appl. Mater. Interfaces 2015, 7, 10258−10265

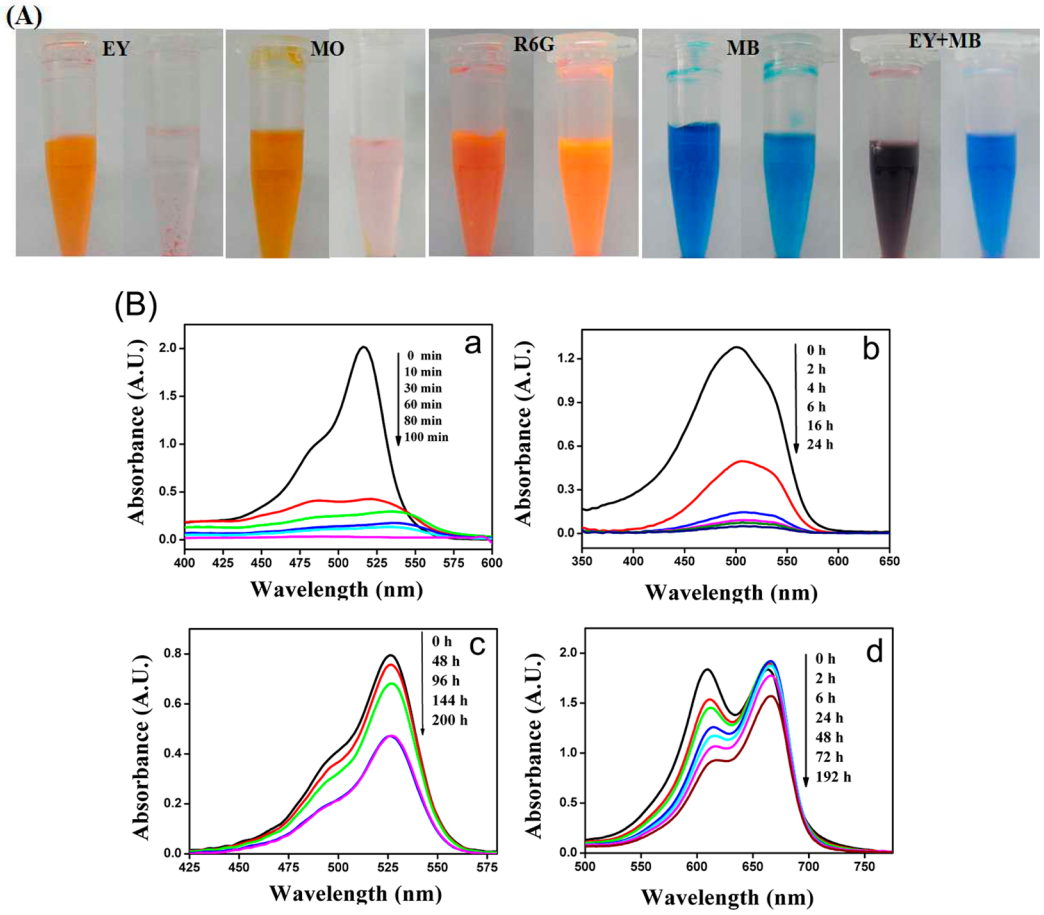

Figure 6. (A) Photos of the dye solutions before (left) and after (right) the removal by the gels; (B) UV−vis spectra of the dye solutions incubated with the gels: EY (a), MO (b), R6G (c) and MB (d) for the indicated time. The solutions for R6G were diluted 5 times before the measurement.

composition of the gel was 20 wt % [*N*-C_{16}, *N*′-CO_2H-Im]Br in DMSO/H_2O (40/60, wt/wt) mixed solvents.

As shown in Figure 6A, EY and MO were efficiently removed after the indicated time, whereas the removals of R6G and MB were not obviously observed. The UV−vis spectroscopy was applied to monitor the removal of dyes at various time intervals (Figure 6B). As shown in Figure 6B-a, with the gels submerged in the aqueous solution of EY, the removal efficiency was remarkable. The concentration of EY decreased sharply, and 80% of the dye was removed after only 10 min of incubation. Furthermore, the dye could not be observed after 100 min, leaving crystal clear water (Figure 6A). We found that the gels showed a faster removal process for EY than other adsorbents reported in previous reports.[13,29,30] The gels were also capable of removing almost all MO molecules from the aqueous solution after 24 h of incubation (Figure 6A,B-b), which is also more efficient than other adsorbents.[31]

On the basis of the UV−vis spectra in Figure 6B-c,-d, although the gels could partially remove R6G and MB dyes after a long time, the efficiency is much lower than that of EY and MO. These results indicate that the gels are very efficient in the removal of anionic dyes such as EY and MO, but have poor elimination capacity for cationic dyes such as R6G and MB. In addition, we found that when an aqueous solution of MB mixed together with four different anionic dyes (EY, acid chrome blue K (ACBK), amido black 10B (AB10B), and chrome azurol S (CAS)) was incubated with the gels, selective removal of the anionic dyes was obviously observed (SI Figure S2). The chemical structures of ACBK, AB10B, and CAS are shown in SI Figure S3. These results also support the selective removal of the anionic dyes by using the constructed gels.

Because the gel system can remove EY completely after 100 min and has a slower removal process for MO, we also examined whether this system could be used to selectively remove anionic dyes. In view of the position of absorption peaks in the UV−vis spectra of dyes, we chose a hydrosoluble dye, AB10B, and attempted to selectively remove the mixture of it with EY (with the same concentration of 0.25 mM in the aqueous solution). The time-dependent removal of AB10B is displayed in SI Figure S4a. We also found that the concentration of AB10B decreased by just 13% after 10 min, whereas the concentration of EY decreased by 80% (SI Figure S4b). In other words, the content of AB10B in the mixed dye solution increased from 50% to 81% after only 10 min. These results demonstrate anionic dyes could be selectively removed.

The selective removal for the anionic dyes exhibited by the gel system is probably related to the electrostatic interaction between the positive center of the imidazolium cation in the adsorbent and the carboxylate or sulfonate anion group of EY or MO, respectively. After incubation in EY solution, we collected the EY-loaded gel on the gel surface and conducted the Fourier transform IR (FTIR) spectra (SI Figure S5). The electrostatic interaction between EY and gelator was evidenced by the red shift of the vibration band of the aromatic imidazolium ring from 1561 to 1541 cm^{-1}.[32] EY exhibits an absorption peak at 1615 cm^{-1}, which is attributed to the

DOI: 10.1021/acsami.5b00814
ACS Appl. Mater. Interfaces 2015, 7, 10258−10265

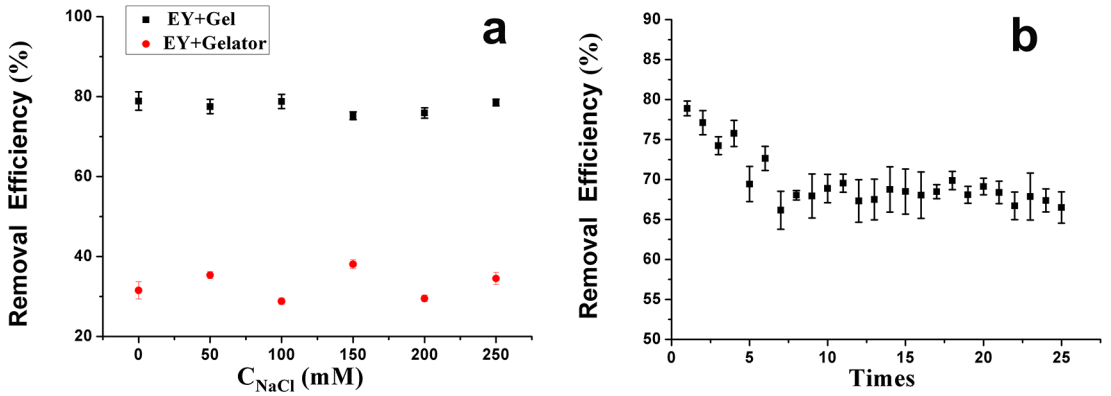

Figure 7. (a) Effect of ionic strength on the removal efficiency of EY in the gel system and (b) removal efficiency as repeated for multiple times.

coupled O−C−O asymmetric stretch of carboxyl group.[33] For the EY-loaded gel, the O−C−O asymmetric stretch band presents a blue shift to 1622 cm^{-1}. Because the chelating mode has a higher wavenumber when the O−C−O angle becomes smaller,[34] it demonstrates EY molecules are anchored onto the gel surface through an ester-like linkage of the carboxyl group of EY.

As one can see from SI Figure S6, the adsorption occurs on the surface of the gel with some precipitation showing. The precipitation might be caused by the gelator slightly dissolved in the water. To verify this assumption, we mixed the saturated solution of gelator with the solution of EY (final concentration, 0.25 mM). After 10 min, the removal efficiency reached 45% (SI Figure S7), and precipitation then appeared. This phenomenon suggests that during the adsorption process by the gel, the dye can also be precipitated by the slightly dissolved gelator in the water simultaneously. As depicted in Figure 6B-a, with increasing time, the band at 515 nm shifted to 538 nm with a broader half-bandwidth. This might be ascribed to $\pi-\pi$ stacking interactions between EY molecules during the precipitation process. This observation is in agreement with previous reports that the $\pi-\pi$ interactions lead to a red shift of EY.[35,36]

On the basis of the above results, an anionic dye removal model could be proposed. Taking EY as an example, some dyes are adsorbed on the surface of the gel through electrostatic interaction between the positive center of the imidazolium cation and the carboxylate of EY. At the same time, a partial of EY and [*N*-C_{16}, *N*′-CO_2H-Im]Br molecules in the solution can aggregate into irregular precipitates, mainly by electrostatic interaction between EY and [*N*-C_{16}, *N*′-CO_2H-Im]Br molecules, $\pi-\pi$ interaction among the aromatic dyes, and hydrophobic interaction provided by cetyl chain of gelators. These driving forces for the formation of the aggregation have been investigated using [*N*-C_{10}, *N*′-CO_2H-Im]Br and anionic congo red (CR) to fabricate the supramolecular materials.[37]

Effect of Ionic Strength and Regenerability of the Adsorbent. Generally, waste waters always contain high-concentration salts, which may significantly affect the performance of the gels. In this section, the effect of ionic strength on the removal efficiency of EY was studied according to the UV−vis spectra of the dye solution. As seen in Figure 7a, an increase in the ionic strength has a negligible effect on the removal efficiency of the dye molecule, even when the concentration of NaCl in the solution is 1000 times higher than that of EY. We also investigated the influence of ionic strength on the removal efficiency of EY by saturated gelator solution, (Figure 7a) and found that the removal efficiency was also independent of the NaCl concentration when the concentration was 1000 times higher than that of EY.

To investigate the recyclability of the gel, the freshly prepared gels were immersed into the aqueous solution of EY (1 mL, 0.25 mM). After 10 min of incubation, the dye solution was measured using UV−vis spectroscopy. Subsequently, 5 mL of deionized water was used to refresh the gel surface before the next adsorption. The recycles were repeated for 25 times, and the gel sample still maintained the original appearance with no visual deformation. We measured the mechanical strength of the above sample and found that the value of G' and G'' still remained at $\sim 10^4$ Pa (SI Figure S8). As depicted in Figure 7b, the removal efficiency decreased initially. After about 7 times, a plateau region was obtained with a nearly constant removal efficiency at about 68%. At equilibrium, adsorption sites on the gel surface are occupied completely, and no further adsorption can occur. Further dye removal capability of the gels can then be attributed to the precipitation of dye molecules with the dissolved gelator in the solution that has low solubility in the solution. Therefore, the performance of the constructed gels will be largely unaffected for long-term water treatment applications. Because the formation of precipitation that is not affected by the ionic strength accounts for most of the total removal efficiency, the gel system in our study could tolerate high-concentration salts, which is an important feature for practical applications in water treatment. We have to point out that for long-term performance or larger water volumes, the application of the constructed gels might be slightly affected by the potential solvent exchange for the real water purification. However, because of the excellent dye removal ability of these gels, they could still be a potent candidate in industrial multistep water purification processes.

CONCLUSIONS

In conclusion, this work describes a self-assembly gel constructed by [*N*-C_{16}, *N*′-CO_2H-Im]Br in a mixture of DMSO/H_2O and studies its efficiency and selectivity as a dye adsorbent. SEM and POM images reveal a microplatelet morphology of the birefringent gels. The strong mechanical strength ensures the gels could be readily regenerated for multiple applications. The $\pi-\pi$ interactions, H-bondings, and hydrophobicity were determined to be the main driving forces for the gelation. Furthermore, the efficient and selective removal of the toxic dyes and recyclability for the gel indicate its potential applications for adsorption, separation, and purification purposes. The removal efficiency might be further

DOI: 10.1021/acsami.5b00814
ACS Appl. Mater. Interfaces 2015, 7, 10258−10265

enhanced by using supramolecular gels with nanoparticle sizes or nanoporous networks; this type of investigation is currently ongoing.

■ ASSOCIATED CONTENT

Supporting Information

Geometry of monomer [*N*-C_{16}, *N*′-CO_2H-Im]Br and packing model of [*N*-CH_3, *N*′-CO_2H-Im]Br; illustration of the removal process; molecular structures of the additionally studied dyes; mixture of dyes before and after the adsorption by the gels; FT-IR spectra; strain sweep lines for the gel sample after 25 reuses. The Supporting Information is available free of charge on the ACS Publications website at DOI: 10.1021/acsami.5b00814.

■ AUTHOR INFORMATION

Corresponding Author

*Phone: +86-531-88364807. Fax: +86-531-88564750. E-mail: ylmlt@sdu.edu.cn.

Notes

The authors declare no competing financial interest.

■ ACKNOWLEDGMENTS

This work was supported by the National Natural Science Foundation of China (No. 21373128), Scientific and Technological Projects of Shandong Province of China (No. 2014GSF117001), the Natural Science Foundation of Shandong Province of China (No. ZR2011BM017), and the Project of Sinopec (No. P13045).

■ REFERENCES

(1) Ali, I. New Generation Adsorbents for Water Treatment. *Chem. Rev.* **2012**, *112*, 5073−5091.
(2) Crini, G. Non-Conventional Low-Cost Adsorbents for Dye Removal: A Review. *Bioresour. Technol.* **2006**, *97*, 1061−1085.
(3) Haque, E.; Jun, J. W.; Jhung, S. H. Adsorptive Removal of Methyl Orange and Methylene Blue from Aqueous Solution with a Metal-Organic Framework Material, Iron Terephthalate (MOF-235). *J. Hazard. Mater.* **2011**, *185*, 507−511.
(4) Chacón-Patiño, M. L.; Blanco-Tirado, C.; Hinestroza, J. P.; Combariza, M. Y. Biocomposite of Nanostructured MnO_2 and Fique Fibers for Efficient Dye Degradation. *Green Chem.* **2013**, *15*, 2920−2928.
(5) Deng, S.; Xu, H.; Jiang, X.; Yin, J. Poly(vinyl alcohol) (PVA)-enhanced Hybrid Hydrogels of Hyperbranched Poly(ether amine) (hPEA) for Selective Adsorption and Separation of Dyes. *Macromolecules* **2013**, *46*, 2399−2406.
(6) Litter, M. Introduction to Photochemical Advanced Oxidation Processes for Water Treatment. In *Environmental Photochemistry, Part II*; Boule, P., Bahnemann, D. W., Robertson, P. K. J., Eds.; Springer: Berlin, Heidelberg, 2005; Vol. *2M*, pp 325−366.
(7) Deng, S.; Wang, R.; Xu, H.; Jiang, X.; Yin, J. Hybrid Hydrogels of Hyperbranched Poly(ether amine)s (hPEAs) for Selective Adsorption of Guest Molecules and Separation of Dyes. *J. Mater. Chem.* **2012**, *22*, 10055−10061.
(8) Li, B.; Jiang, X.; Yin, J. Multi-Responsive Microgel of Hyperbranched Poly(ether amine) (hPEA-mGel) for the Selective Adsorption and Separation of Hydrophilic Fluorescein Dyes. *J. Mater. Chem.* **2012**, *22*, 17976−17983.
(9) George, M.; Weiss, R. G. Molecular Organogels. Soft Matter Comprised of Low-Molecular-Mass Organic Gelators and Organic Liquids. *Acc. Chem. Res.* **2006**, *39*, 489−497.
(10) Weiss, R. G. The Past, Present, and Future of Molecular Gels. What Is the Status of the Field, and Where Is It Going? *J. Am. Chem. Soc.* **2014**, *136*, 7519−7530.
(11) Buerkle, L. E.; Rowan, S. J. Supramolecular Gels Formed from Multi-Component Low Molecular Weight Species. *Chem. Soc. Rev.* **2012**, *41*, 6089−6102.
(12) Okesola, B. O.; Smith, D. K. Versatile Supramolecular pH-Tolerant Hydrogels which Demonstrate pH-Dependent Selective Adsorption of Dyes from Aqueous Solution. *Chem. Commun.* **2013**, *49*, 11164−11166.
(13) Bairi, P.; Roy, B.; Nandi, A. K. pH and Anion Sensitive Silver (I) Coordinated Melamine Hydrogel with Dye Absorbing Properties: Metastability at Low Melamine Concentration. *J. Mater. Chem.* **2011**, *21*, 11747−11749.
(14) Wang, X.; Yu, L.; Jiao, J.; Zhang, H.; Wang, R.; Chen, H. Aggregation Behavior of COOH-Functionalized Imidazolium-Based Surface Active Ionic Liquids in Aqueous Solution. *J. Mol. Liq.* **2012**, *173*, 103−107.
(15) Frisch, M. J.; Trucks, G. W.; Schlegel, H. B.; Scuseria, G. E.; Robb, M. A.; Cheeseman, J. R.; Scalmani, G.; Barone, V.; Mennucci, B.; Petersson, G. A.; Nakatsuji, H.; Caricato, M.; Li, X.; Hratchian, H. P.; Izmaylov, A. F.; Bloino, J.; Zheng, G.; Sonnenberg, J. L.; Hada, M.; Ehara, M.; Toyota, K.; Fukuda, R.; Hasegawa, J.; Ishida, M.; Nakajima, T.; Honda, Y.; Kitao, O.; Nakai, H.; Vreven, T.; Montgomery, J. A., Jr.; Peralta, J. E.; Ogliaro, F.; Bearpark, M.; Heyd, J. J.; Brothers, E.; Kudin, K. N.; Staroverov, V. N.; Kobayashi, R.; Normand, J.; Raghavachari, K.; Rendell, A.; Burant, J. C.; Iyengar, S. S.; Tomasi, J.; Cossi, M.; Rega, N.; Millam, N. J.; Klene, M.; Knox, J. E.; Cross, J. B.; Bakken, V.; Adamo, C.; Jaramillo, J.; Gomperts, R.; Stratmann, R. E.; Yazyev, O.; Austin, A. J.; Cammi, R.; Pomelli, C.; Ochterski, J. W.; Martin, R. L.; Morokuma, K.; Zakrzewski, V. G.; Voth, G. A.; Salvador, P.; Dannenberg, J. J.; Dapprich, S.; Daniels, A. D.; Farkas, O.; Foresman, J. B.; Ortiz, J. V.; Cioslowski, J.; Fox, D. J. *Gaussian 09, version A.02*; Gaussian, Inc.: Wallingford, CT, 2009.
(16) Hohenstein, E.; Chill, S.; David Sherrill, C. Assessment of the Performance of the M05-2X and M06-2X Exchange-Correlation Functionals for Noncovalent Interactions in Biomolecules. *J. Chem. Theory Comput.* **2008**, *4*, 1996−2000.
(17) Papajak, E.; TruhlarEfficient, D. Diffuse Basis Sets for Density Functional Theory. *J. Chem. Theory Comput.* **2010**, *6*, 597−601.
(18) Tomasi, J.; Mennucci, B.; Cammi, R. Quantum Mechanical Continuum Solvation Models. *Chem. Rev.* **2005**, *105*, 2999−3093.
(19) Pal, A.; Abraham, S.; Rogers, M. A.; Dey, J.; Weiss, R. G. Comparison of Dipolar, H-Bonding, and Dispersive Interactions on Gelation Efficiency of Positional Isomers of Keto and Hydroxy Substituted Octadecanoic Acids. *Langmuir* **2013**, *29*, 6467−6475.
(20) Jin, Q.; Zhang, L.; Liu, M. Solvent-Polarity-Tuned Morphology and Inversion of Supramolecular Chirality in a Self-Assembled Pyridylpyrazole-Linked Glutamide Derivative: Nanofibers, Nanotwists, Nanotubes, and Microtubes. *Chem.—Eur. J.* **2013**, *19*, 9234−9241.
(21) Weng, W.; Li, Z.; Jamieson, A. M.; Rowan, S. J. Control of Gel Morphology and Properties of a Class of Metallo-Supramolecular Polymers by Good/Poor Solvent Environments. *Macromolecules* **2008**, *42*, 236−246.
(22) Cheng, N.; Hu, Q.; Bi, Y.; Xu, W.; Gong, Y.; Yu, L. Gels and Lyotropic Liquid Crystals: Using an Imidazolium-Based Catanionic Surfactant in Binary Solvents. *Langmuir* **2014**, *30*, 9076−9084.
(23) Ballabh, A.; Adalder, T. K.; Dastidar, P. Structures and Gelation Properties of a Series of Salts Derived from an Alicyclic Dicarboxylic Acid and *n*-Alkyl Primary Amines. *Cryst. Growth Des.* **2008**, *8*, 4144−4149.
(24) Abdallah, D. J.; Sirchio, S. A.; Weiss, R. G. Hexatriacontane organogels. The First Determination of the Conformation and Molecular Packing of a Low-Molecular-Mass Organogelator in Its Gelled State. *Langmuir* **2000**, *16*, 7558−7561.
(25) Krieg, E.; Shirman, E.; Weissman, H.; Shimoni, E.; Wolf, S. G.; Pinkas, I.; Rybtchinski, B. Supramolecular Gel Based on a Perylene Diimide Dye: Multiple Stimuli Responsiveness, Robustness, and Photofunction. *J. Am. Chem. Soc.* **2009**, *131*, 14365−14373.
(26) Abraham, S.; Lan, Y.; Lam, R. S. H.; Grahame, D. A. S.; Kim, J. J. H.; Weiss, R. G.; Rogers, M. A. Influence of Positional Isomers on the Macroscale and Nanoscale Architectures of Aggregates of Racemic

DOI: 10.1021/acsami.5b00814
ACS Appl. Mater. Interfaces 2015, 7, 10258−10265

Hydroxyoctadecanoic Acids in Their Molecular Gel, Dispersion, and Solid States. *Langmuir* **2012**, *28*, 4955−4964.
(27) Appaw, C.; Gilbert, R. D.; Khan, S. A.; Kadla, J. F. Viscoelastic Behavior of Cellulose Acetate in a Mixed Solvent System. *Biomacromolecules* **2007**, *8*, 1541−1547.
(28) Horinaka, J.-i.; Yasuda, R.; Takigawa, T. Rheological Properties of Concentrated Solutions of Agarose in Ionic Liquid. *J. Appl. Polym. Sci.* **2012**, *123*, 3023−3027.
(29) Du, W. L.; Xu, Z. R.; Han, X. Y.; Xu, Y. L.; Miao, Z. G. Preparation, Characterization and Adsorption Properties of Chitosan Nanoparticles for Eosin Y As a Model Anionic Dye. *J. Hazard. Mater.* **2008**, *153*, 152−156.
(30) Chatterjee, S.; Chatterjee, S.; Chatterjee, B. P.; Das, A. R.; Guha, A. K. Adsorption of a Model Anionic Dye, Eosin Y, from Aqueous Solution by Chitosan Hydrobeads. *J. Colloid Interface Sci.* **2005**, *288*, 30−35.
(31) Mittal, A.; Malviya, A.; Kaur, D.; Mittal, J.; Kurup, L. Studies on the Adsorption Kinetics and Isotherms for the Removal and Recovery of Methyl Orange from Wastewaters Using Waste Materials. *J. Hazard. Mater.* **2007**, *148*, 229−240.
(32) Malek, K.; Puc, A.; Schroeder, G.; Rybachenko, V. I.; Proniewicz, L. M. FT-IR and FT-Raman Spectroscopies and DFT Modelling of Benzimidazolium Salts. *Chem. Phys.* **2006**, *327*, 439−451.
(33) Meyer, T. J.; Meyer, G. J.; Pfening, B. W.; Schoonover, J. R.; Timpson, C. J.; Wall, J. F.; Kobusch, C.; Chen, X.; Peek, B. M. Molecular-Level Electron Transfer and Excited State Assemblies on Surfaces of Metal Oxides and Glass. *Inorg. Chem.* **1994**, *33*, 3952−3964.
(34) Couzis, A.; Gulari, E. Adsorption of Sodium Laurate from Its Aqueous Solution onto an Alumina Surface. A Dynamic Study of the Surface-Surfactant Interaction Using Attenuated Total Reflection Fourier Transform Infrared Spectroscopy. *Langmuir* **1993**, *9*, 3414−3421.
(35) Rossetti, R.; Brus, L. E. Time-Resolved Raman Scattering Study of Adsorbed, Semioxidized Eosin Y Formed by Excited-State Electron Transfer into Colloidal Titanium (IV) Oxide Particles. *J. Am. Chem. Soc.* **1984**, *106*, 4336−4340.
(36) Mou, Z.; Dong, Y.; Li, S.; Du, Y.; Wang, X.; Yang, P.; Wang, S.; Eosin, Y. Functionalized Graphene for Photocatalytic Hydrogen Production from Water. *Int. J. Hydrogen Energy* **2011**, *36*, 8885−8893.
(37) Gong, Y. J.; Hu, Q. Z.; Cheng, N.; Wang, T.; Xu, W. W.; Bi, Y. H.; Yu, L. Fabrication of pH- and Temperature-Directed Supramolecular Materials from 1D Fibers to Exclusively 2D Planar Structures Using an Ionic Self-Assembly Approach. *J. Mater. Chem.* **2015**, *3*, 3273−3279.

DOI: 10.1021/acsami.5b00814
ACS Appl. Mater. Interfaces 2015, 7, 10258−10265